We are IntechOpen, the world's leading publisher of Open Access books Built by scientists, for scientists

6,900
Open access books available

186,000
International authors and editors

200M
Downloads

Our authors are among the

154
Countries delivered to

TOP 1%
most cited scientists

12.2%
Contributors from top 500 universities

CLARIVATE ANALYTICS
BOOK CITATION INDEX
INDEXED

WEB OF SCIENCE™

Selection of our books indexed in the Book Citation Index
in Web of Science™ Core Collection (BKCI)

Interested in publishing with us?
Contact book.department@intechopen.com

Phase Diagram Analysis for Predicting Nonlinearities and Transient Responses

Juan Carlos Jáuregui
CIATEQ, A.C.
Mexico

1. Introduction

The developments of new manufacturing processes have impacted modern machinery. Nowadays, mechanical parts are produced with tighter tolerances that allow very high precise assemblies. On the other hand, new materials and design techniques have developed lighter elements. Thus, modern machinery operates at very high speeds and accelerations, which, in many cases, shows nonlinear dynamic behaviors.

Intelligent manufacturing systems require on line monitoring equipment coordinated by the control systems. Traditionally, monitoring systems are based on the Fast Fourier Transform (FFT), which, due to its basis is unable to identify transient responses, and nonlinear behaviors. On the other hand, the FFT requires a considerable processing time that limits its application to early fault detections. The development of new sensors, signal processing techniques and faster microprocessors are key elements for modern monitoring systems. These systems require a better understanding of the machine response and the nature of the output signals.

The evolution of the phase space, or phase diagram, represents how the dynamic system evolves in time. Nonlinearities and transient responses can be determined from the smoothness of the tangent vector of the phase diagram accordingly to Liouville's theorem.

Therefore, the phase diagram is a useful technique for predicting transient and nonlinear behavior in mechanical systems. Even more, the phase diagram can be implemented electronically for on line monitoring, and it can identify faults in real time.

Mathematical modeling refers to the use of mathematical language to simulate the behavior of a system. Its role is to provide a better understanding and characterization of the system. In the theory of mechanical vibrations, mathematical models are helpful for the analysis of dynamic behavior of the structure being modeled (Kerschen et al. 2006). Even with advanced computers, experimental testing and system identification help designers to evaluate numerical predictions with experimental data. The term "system identification" is sometimes used in a broader context and may also refer to the extraction of information about the structural behavior directly from experimental data. In this case, it is referred as any systematic way of deriving models from experimental data. This is the main objective of any machinery monitoring systems (Masri 1994).

For linear systems, modal analysis is the most popular approach for system identification. It can describe the behavior of a system for any input. Examples of this are: Ibrahim time domain method, eigensystem realization algorithm, stochastic subspace identification method, polyreference least-square complex frequency domain method among others.

In structural dynamics, typical sources of nonlinearities are:
- Large displacements, large deformations
- Inertia nonlinearities
- Material nonlinearities
- Dry friction effects
- Boundary conditions

Also, viscoelastic supports show marked nonlinear behavior. And it is quite common to find nonlinearities in a damaged structure. Even though, these are two sources of nonlinearities, viscoelastic supports have a stable response, whereas a damaged structure will developed a drastic change in the system's stiffness that can show jumps and chaos.

As it was stated before, there is a need for designing lighter and more flexible machinery and structures. The basic principles that apply to a linear system, and that are the basis for modal analysis, are no longer valid. These phenomena include jumps, bifurcations, saturation, subharmonics, superharmonics, internal resonances, limit cycles, modal interactions and chaos.

One of the ways to study nonlinear systems is the linearization approach. Weakly nonlinear systems were analyzed using the perturbation theory which includes averaging, Lidsteadt-Poincare technique and the method of multiple scales. There are new methodologies such as nonlinear energy pumping, (Wiercigroch & Pavlovskaia, 2008). In particular, nonlinear normal modes (NNMs) and nonlinear multi-modes (NMMs) have been constructed by using the method of multiple scales. This is to analyze the vibration responses by monitoring the modal responses and mode interactions.

The development of structural models from experimental measurements requires methods such as "nonlinear system identification". There is a significant difference from the linear systems, each nonlinear structure has a unique nature, and thus it is very difficult to have a general method to describe a nonlinear system. Therefore, for every type of nonlinearity a different method is required.

An example of a nonlinear system is the Duffing oscillator; it represents a typical example of a polynomial form of restoring force, whereas hysteric damping is an example of a non-polynomial form of nonlinearity. This represents a major difficulty since there is not a single model (Pai, 2007; Li & Qu, 2007).

In a nonlinear system, its stiffness cannot be easily identified. They proposed to estimate the dynamic behavior from the stochastic response. The period of a free oscillation depends on the energy level. Rüdinger & Krenk (2001) determined the dynamic parameters of a simple nonlinear system (equivalent to a nonlinear oscillator).

An area of major interest is the application of simulation technique to nonlinear system identification. There are a vast number of techniques that have been applied to this topic. Most of them are developed from the identification of uncertain quantities. Monte Carlo simulation is a universal method that can provide accurate solutions for problems involving nonlinearities (Schuëller 1997). The major advantage on Monte Carlo simulation is that accurate solutions can be obtained for any problem whose deterministic solution is known. The disadvantage is that it is time-consuming. The most important part is the generation of sample functions of the stochastic process:
- Stationary or non-stationary
- Homogenous or non-homogeneous
- One dimensional or multidimensional
- Single variable or multivariable

- Gaussian or non-Gaussian

For the nonlinear system identification techniques, there are two broad categories: parametric and non-parametric methods.

Parametric methods assume that the system is represented by a mathematical model. Identification consists on the estimation of the model parameters from the experimental data. ($\ddot{x} + \zeta\dot{x} + \omega^2 x = f(t)$ ω and ζ are estimated). These methods also allow for the design verification.

Nonparametric methods refer to techniques which lack of a mathematical model. They take a "system" approach and fit the input-output relationship. (Examples: Auto-Regressive-Moving-Average, Volterra Wiener-Kerner, etc.) Their limitations are the type of input signals, they required many parameters to find a solution. The model could introduce errors that are not related to the system, and noise measurements could be introduced into the model parameters. This is the main source of uncertainty.

Masri (1994) developed a hybrid approach for the identification of nonlinear systems. He applied a parametric approach for the identification of the linear terms and the well know nonlinear terms, and a parametric approach for describing the unknown nonlinear terms.

The approximation is defined from the equation of motion as:

$$M(\ddot{x}) + C(\dot{x}) + K(x) + f_N(t) = f(t),\tag{1}$$

where $f_N(t)$ includes the nonlinear non-conservative forces

$$f_N(t) = f(t) - M(\ddot{x}) - C(\dot{x}) - K(x).\tag{2}$$

The right hand side can be determined from a parametric modeling and $f(t)$ is a well known input function.

$f_N(t)$ can be modeled as a combination of parametric and non-parametric term, this is what Masri (1994) described as a hybrid model. He approximated the $f_N(t)$ as vector h were each element $h_i(t)$ is a function of the acceleration, velocity and position vectors associated with each degree of freedom. Masri (1994) showed that the nonlinear terms can be visualized in the phase diagram and they can be isolated by subtracting the linear components from the measured data.

The development of the nonlinear dynamic theory brought new methods for recognition and prediction of nonlinear dynamic response (Yang 2007).

The nonlinear dynamic and chaos theory can be used to describe the irregular, broadband signals, which are generic in non-linear dynamical systems, and extracting some physically interesting and useful features from such signals. Fractal dimension, such as the capacity dimension, correlation dimension, and information dimension, developed by the Nonlinear dynamic and chaos theory, is a promising new tool to interpret observations of physical systems where the time trace of the measured quantities is irregular. The phase diagram and Poincare maps of chaotic systems have a fractal structure. We can recognize, classify and understand such maps of chaos by measuring the stability of the phase diagram.

Vela et al. (2010) applied a detrended fluctuation analysis (DFA), adapted for time–frequency domain, to monitor the evolution nonlinear dynamics. The underlying idea behind the application was to use the Hurst exponent, an index of the signal fractal roughness, to detect dominance of unstable oscillatory components in the complex, presumably stochastic, dynamics of machine acceleration. In early stages of machinery faults the signal-noise ratio is very low due to relatively weak energy signals. Other authors

have studied the effect of a weak periodic signal in the chaotic response of a nonlinear oscillator (Li & Qu, 2007; Modarres et al. 2011). Liu (2005) developed a visualization method for nonlinear chaotic systems.

One of the advantages of the display identification is the representation of the phase diagram as a three-dimensional plot. In this way the phase diagram can be related to the frequency and the dynamic identification of the system. According to Taken's theorem, a dynamic system can be obtained by reconstructing the phase diagram (Wang, G. et al. 2009; Wang, Z., et al. 2011; Ghafari et al. 2010).

Karpenko et al., (2006) applied the phase diagram in the identification of nonlinear behavior of rotors. They also demonstrated that rubbing is nonlinear and can be identified as a chaotic system. Mevela &. Guyade (2008) developed a model for predicting bearing failures.

In this chapter, the application of the phase space, or phase diagram, to the identification of nonlinearities and transient function is presented. The theoretical background is discussed in next section, and afterwards its application to the most relevant mechanical systems is presented.

2. Phase diagram definition

The analysis and modeling of dynamic systems can be done from a Lagrangian approach or from a Hamiltonian approach. The Lagrangian approach describes how position and velocity change in time. The Hamiltonian approach describes how position and momentum change in time. The position and momentum of a particle specifies a point in a space called the "phase space", "phase plane", "phase diagram", among others (Nichols, 2003).

A particle traces out a path in a space R^n

$$q: \mathcal{R} \to \mathcal{R}^n \tag{3}$$

where R represents time domain, R^n represents the space domain and q represents the position of a particle at an instant t.

From Newton's law

$$F(t) = \frac{d}{dt}\big(m\dot{q}(t)\big) = \frac{d}{dt}(p(t)), \tag{4}$$

with the restriction that $F(t)$ is a smooth function.

The potential energy of a multi-particle system will have the form

$$V_i(t) = \sum_{i \neq j} V_{ij}\big|q_i(t) - q_j(t)\big| \tag{5}$$

where

$$V_{ij} = -\int_c^r f_{ij}(s)\,ds \tag{6}$$

and f_{ij} is the force acting between particle i and j.

Hamilton's principle is defined as:

$$H(q,p) = \frac{p^2}{2m} + V(q) \tag{7}$$

and

$$\frac{\partial H(q,p)}{\partial p_i} = \frac{p_i}{m} \tag{8}$$

$$\frac{\partial H(q,p)}{\partial q_i} = \frac{\partial V(q)}{\partial q}. \tag{9}$$

Thus

$$\frac{d}{dt}q_i(t) = \frac{\partial H}{\partial p_i}(q(t),p(t)) \tag{10}$$

$$\frac{d}{dt}p_i(t) = -\frac{\partial H}{\partial q_i}(q(t),p(t)),$$

where the dyad $(q(t),p(t))$ represents the phase space of a particle, and $(q,p) \in \mathcal{R}^n x \mathcal{R}^n$.
If the phase space can be represented as a smooth function $\varphi: \mathcal{R}^n x \mathcal{R}^n \to \mathcal{R}$, then it represents the system's evolution in time. Thus, for a system with n particles

$$\frac{d\varphi}{dt} = \sum_i \frac{\partial \varphi}{\partial q_i}\frac{dq_i}{dt} + \frac{\partial \varphi}{\partial p_i}\frac{dp_i}{dt}. \tag{11}$$

Using Hamilton's equation

$$\frac{d\varphi}{dt} = \sum_i \frac{\partial \varphi}{\partial q_i}\frac{\partial H}{\partial p_i} - \frac{\partial \varphi}{\partial p_i}\frac{\partial H}{\partial q_i} \tag{12}$$

For example, a simple harmonic is represented as

$$m\ddot{q}(t) + kq(t) = 0 \tag{13}$$

with its well known solution

$$q(t) = Asin(\omega t) + Bcos(\omega t) \tag{14}$$

$$p(t) = m(A\omega cos(\omega t) - B\omega sin(\omega t)) \tag{15}$$

where

$$A = q(0) \tag{16}$$

$$B = \frac{p(0)}{m}.$$

The Hamiltonian can be written as:

$$H(q,p) = \frac{1}{2}\left(\frac{p^2}{m} + kq^2\right). \tag{17}$$

The field vector operator is defined as:

$$v_H = p\frac{\partial}{\partial q} - q\frac{\partial}{\partial p} \tag{18}$$

and the flow field is found as:

$$\varphi_t = [q(t),p(t)]. \tag{19}$$

In this case

$$\varphi_t = \left[q(0)\sin(\omega t) + \frac{p(0)}{m}\cos(\omega t) , q(0)m\omega\cos(\omega t) - p(0)\omega\sin(\omega t) \right] \tag{20}$$

This flow field represents an ellipse at any time *t*.

The dynamic stability is determined from Liouville's theorem, (the phase space volume occupied by a collection of systems evolving according to Hamilton's equations of motion will be preserved in time):

$$\frac{dH}{dt} = \frac{\partial H}{\partial t} + \sum_{i=1}^{n} \left(\frac{\partial H}{\partial q_i}\dot{q}_i + \frac{\partial H}{\partial p_i}\dot{p}_i \right) = 0 \tag{21}$$

It can be shown that

$$\sum_{i=1}^{n} \left(\frac{\partial^2 H}{\partial q_i \partial p_i} - \frac{\partial^2 H}{\partial q_i \partial p_i} \right) = 0 \tag{22}$$

This conservation law states that a phase diagram volume will be preserved in time; this is the statement of Liouville's theorem.

3. Application to nonlinear mechanical systems

3.1 Gears

As a complete system a gear box contains gears or teeth wheels, shafts, bearings, rolling bearings, lubrication pumps, tubes, valves and other devices such as heat exchangers. Therefore, all these individual elements have gone through a development process by themselves, but as an integrated system they have challenged engineers with highly interesting problems. The one of particular interest is gear vibrations, which is always undesirable, and also generates noise. The dominant cause of gear noise is the Transmission Error; it is the deviation from a perfect motion between the driver and the driven gears. And it is the combination of different gear variations, such as non perfect tooth profiles, pitch errors, elastic deformations, backlash, etc. The simplest type of noise is a steady note which may have a harmonic content at the gear mesh frequency. This frequency is normally modulated by the rotating frequency. Modulated noise is often described as a buzzing sound. In general, gears show a frequency modulated spectrum with a distinguishable mesh frequency and side bands spaced at the shaft rotating frequency. Other noises are associated with pitch errors. They are described as scrunching, grating, grouching, etc. They contain a wide range of frequencies that are a lot higher than the rotating frequency. White noise can also be present and it may be associated with loss of contact between the teeth. (Jauregui & Gonzalez, 2009).

Gear box vibration is a typical nonlinear vibration phenomenon. Its nonlinear behavior comes from the discontinuities in the stiffness of the system, which comes from the combination of two teeth acting in conjunction. Thus, the stiffness of a gear pair varies with the angular position, except in very specific gear designs. One of the main features of gear pair stiffness is that it changes drastically as a function of the number of teeth in simultaneous contact. Ideally, a pair of gears transmits motion at a constant speed.

In most gear pair systems, torsional motion is coupled by the gear pair stiffness; therefore a two degree of freedom model will reflect accurately most practical applications. If it is necessary to include other effects, increasing the degrees of freedom could accommodate other compliances that are present in the system.

Many researchers and engineers have developed a significant number of gear dynamic models. Most of them have been developed for the prediction of noise and vibrations, and they have demonstrated that gear vibrations are highly nonlinear. In this chapter we present one of the most commonly used model that is widely accepted. It was demonstrated that a simplified lumped-mass model is adequate for small transmissions. (Chang 2010).
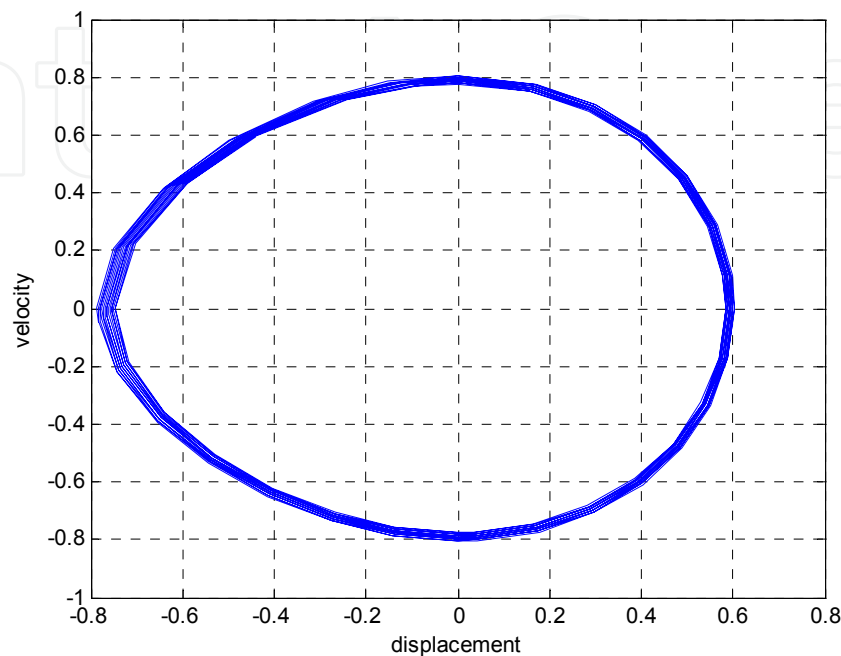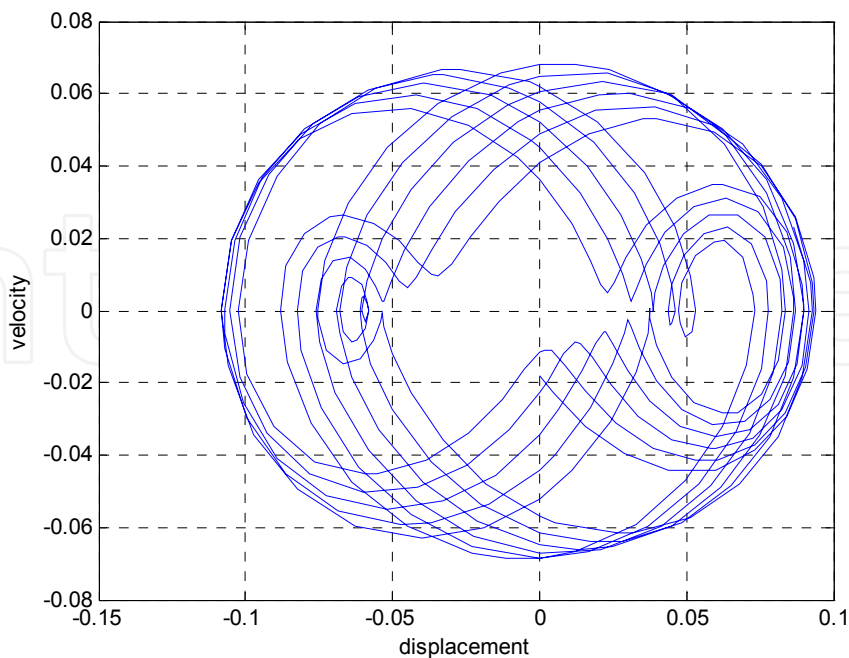

Fig. 1. Phase diagram of a pair of gears under free vibration.

Fig. 2. Phase diagram of a pair of gears with an external excitation of 0.4 of the linear natural frequency

In this case, it is important to identify the effect of the nonlinear gear action in a phase diagram. From a simple lumped mass model, it is sufficient to identify the nonlinear response of a transmission. Fig 1 represents the phase diagram of the free vibration response. In this case, a small damping coefficient was included in the model. It is noticeable how the nonlinear stiffness deforms the phase space pattern, and instead of producing an ellipse, it forms a lemon shape. For practical purposes, this pattern is stable at any time.

Fig. 2, represents the forced vibration response with an external excitation at 0.4 ω_N. It is clear to see how the stable pattern disappears, and two attracting poles are formed around the origin of the phase space. This behavior is similar to a nonlinear Duffing oscillator. Fig. 3 shows the same system but with an external excitation beyond its first linear natural frequency. In this case, the instability is larger and number of attracting poles increases and the velocity amplitude almost doubles the other two cases.

Gears have a characteristic phase diagram; it changes from a stable non-elliptical pattern to a chaotic phase space. This drastic change is quite significant and, with an appropriate monitoring system, it can detect early faults in the gear teeth, or damaging effects caused by changes in the operating conditions.

3.2 Discontinuous stiffness

Stiffness discontinuities are present in many mechanical systems. It is one reason why gears have a nonlinear dynamic behavior. Another type of stiffness discontinuity is found in cracked structures. Andreaus & Baragatti (2011) demonstrated that a cracked beam behaves as a discontinuous stiffness system. This discontinuity is a function of the beam's displacement, thus the stiffness is lower when the beam's movement opens the crack and the stiffness increases when the movement closes the crack. Also large deformations can produce a similar pattern as a system with stiffness discontinuities, (Machado et al. 2009), (Mazzillia et al.,2008).
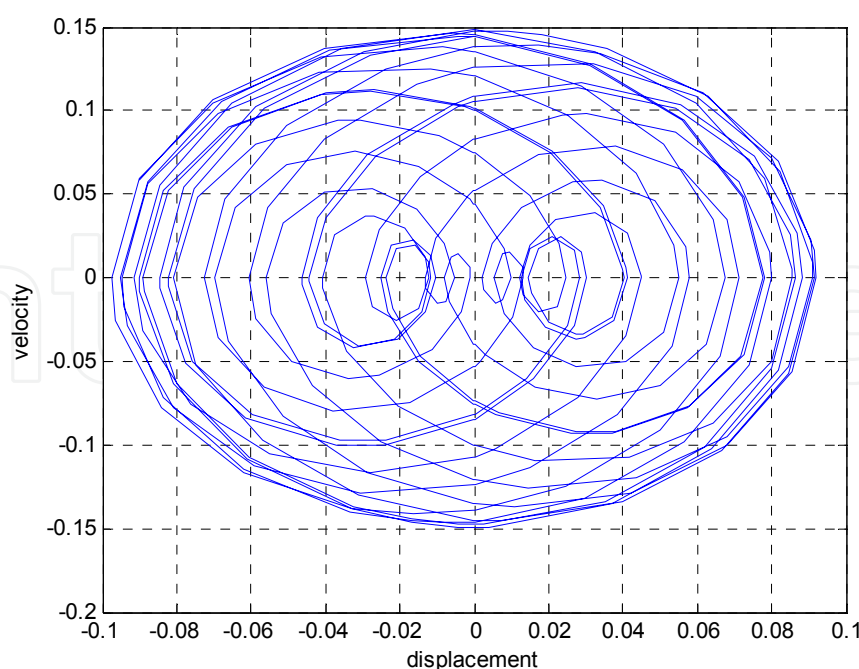

Fig. 3. Phase diagram of a pair of gears with an external excitation of 1.6 of the linear natural frequency

A typical pattern of a beam under large deformations can be seen in Fig. 5 (Jauregui & Gonzalez, 2009b). The elliptic shape evolves into a rectangular shape with two attracting poles.

This behavior is found in very large and thin structures such as wind turbine blades or helicopter blades. The stability of these structures depends entirely on internal damping capabilities.

3.3 Bearings

Most of the dynamic models of rolling bearings consider that their stiffness is a function of the frequency and the displacement. This characteristic makes its dynamic behavior different from other mechanical elements. And, as was stated in the introduction, it is quite complicated to establish a single nonlinear mode of vibration. Thus, in a bearing system, strange motions appear due to the nature of the stiffness function. To describe these strange motions, tools specific to chaotic dynamics have to be introduced. Fourier spectra are convenient for detecting sub- or super-harmonics of a component, also in the case of complete chaotic behavior, but the quasi-periodic motion is impossible to detect except for the ideal case of two components. Some recent studies have used phase diagrams and Poincaré sections. An extremely efficient technique is then to sample the phase diagram points using a convenient clock frequency, in order to obtain a limited number of points. The resulting shape is an excellent tool to characterize sub-harmonic, quasi-periodic or chaotic motions.
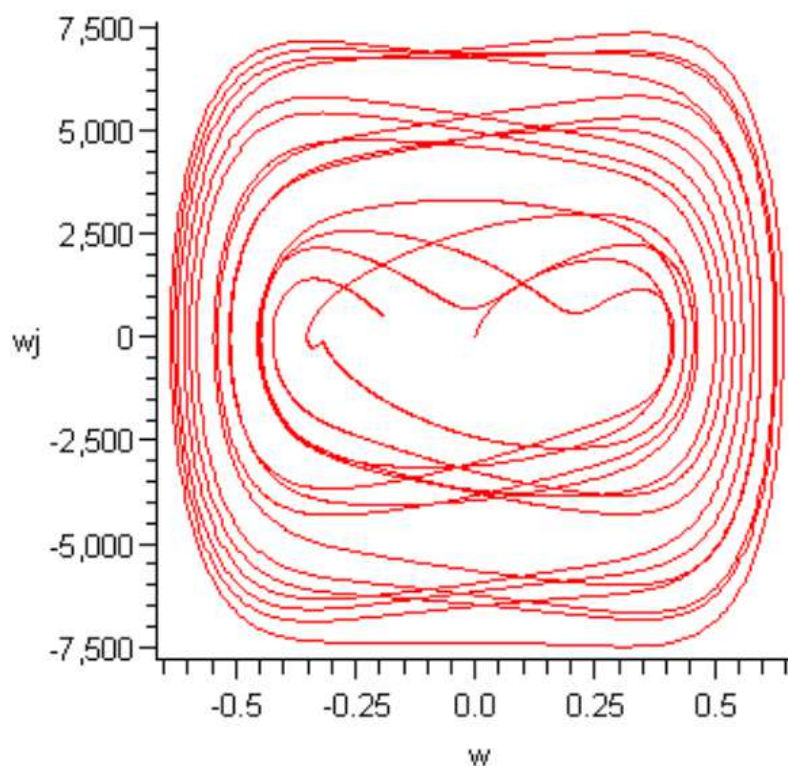

Fig. 5. Phase diagram of a beam under large deformations

A typical ball-bearing system consists of five contact parts: the shaft, the inner ring, the rolling elements, outer ring and the housing. The deformation of each part will influence the

load distribution and, in turn, the service life of the bearing. It is well known that classical calculation methods cannot predict accurately load distributions inside the bearing. Ball bearings (Fig 6) are very stiff compared with sliding bearings; their stiffness can be approximating as a set of individual springs; where the number of springs supporting the shaft varies with the angular position of the shaft. This variation depends upon the kinematics of the ball roller as it moves around the shaft. Thus, the ratio of rotation of the ball as a function of shaft's rotation is determined as

$$\omega_b = \frac{D\omega_s}{d} \tag{24}$$

The fundamental principle of a rolling bearing is that the ball or roller translates around the shaft, eliminating must of the friction; then the ball's angular translation is found as (D is the pitch diameter and d is the roller diameter)

$$\phi = \frac{d\cos(\omega_b t)}{D + \dfrac{d}{2}}\cos(\alpha) \tag{25}$$

The number of balls, or rolls in contact are determined from Fig. 7. The nonlinear characteristic of the rolling bearing is the ball-track deformation. The ball-track stiffness is calculated with the Hertz equation. Since the balls translate around the shaft, the number of balls supporting the load varies with the angular position of the shaft; this translation effect modifies the overall stiffness of the bearing. Although this variation may be small, it creates a nonlinear vibration, which turns out to be relatively difficult to identify in field problems.
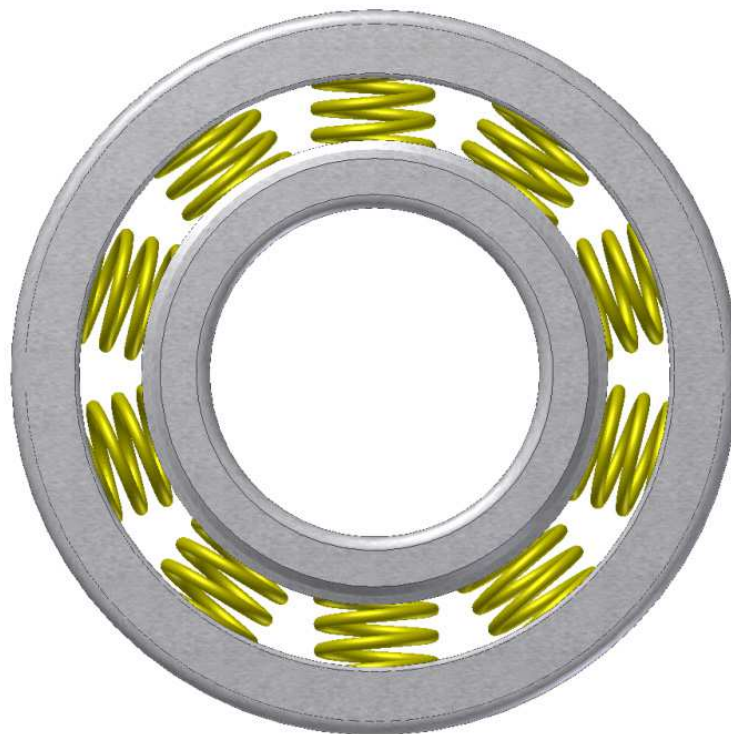

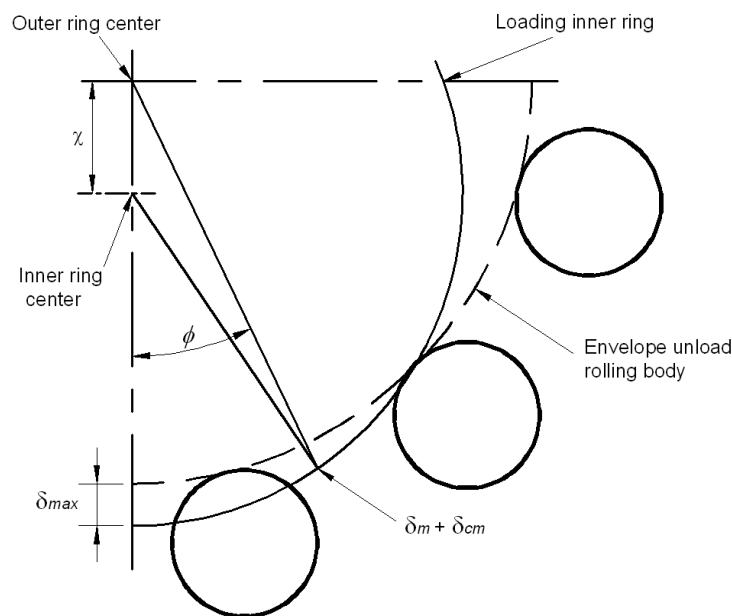Fig. 6. Schematic representation of a roller bearing

Fig. 7. Radial displacement of a shaft mounted on ball bearings

Rolling bearings generate transient vibrations due to stiffness nonlinearities and structural defects. There are four external sources of vibration; two of them are associated with the angular velocity of the ball ω_b and their angular translation ω_ϕ. The other two frequencies are related to structural defects on the inner and outer tracks. These external frequencies excite the nonlinear terms. The stiffness of the ball as a function of the deformation is almost constant:

$$P_i = E\sqrt{\frac{Dd}{(D-d)}\left(\frac{\delta_i}{\alpha_H}\right)^3} \tag{26}$$

The nonlinear effect comes from the combination of balls deformation as they roll around the shaft. The rolling bearing can be modeled as a mass-spring system.

$$\delta_i = \delta_{\max}\cos\left[\frac{\pi}{2}-i\left(\phi+\frac{2(i-1)\pi}{N}\right)\right] \tag{27}$$

The spring stiffness is determined from Fig. 8. Similarly as the gear mesh stiffness, rolling bearings exhibits a periodic function, thus it can be expanded as a Taylor series:

$$k_x = a_0 + a_1\phi + a_2\phi^2 + a_3\phi^3 \tag{28}$$

Coefficients a_i are function of the number of balls under load, and ϕ represents roller translation angle.

The solution of the dynamic model requires the definition of the transmitted force. Ideally, it should be constant, and equal to the radial force. But, it is not the case; first of all, the radial force varies according to every application, and the rolling bearing itself produces a specific type of excitation forces. These forces are associated with physical defects on the bearing, and there are basically four types of excitation.

One of the challenges of a monitoring system is the identification of early faults in rolling bearings. Failures in bearings start at surface level; thus, they generate a relatively small

energy vibration compared to other sources, and its identification is very cumbersome. With the application of phase diagram plots, early failures can be predicted in real time. The process is as follows:
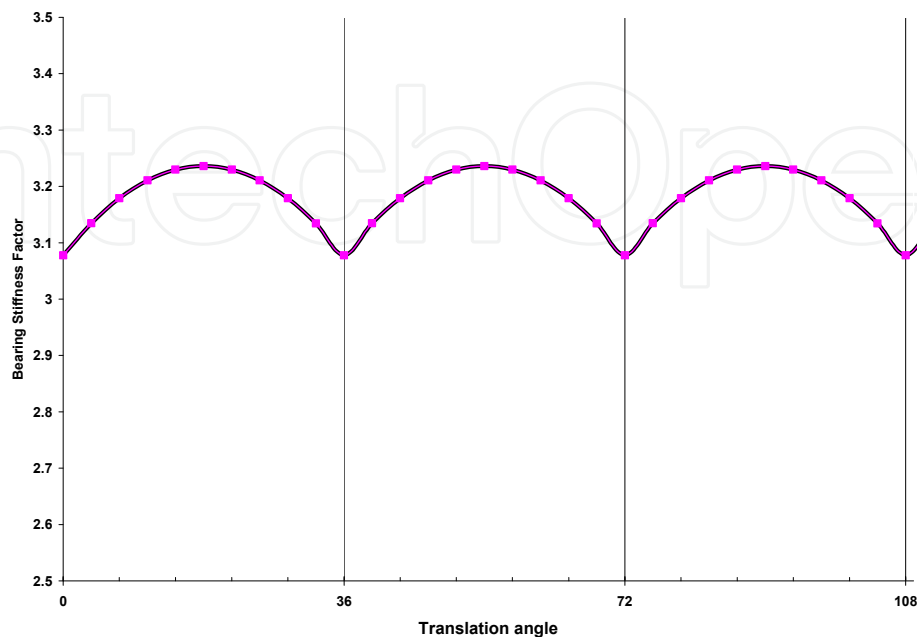

Fig. 8. Bearing stiffness function

Vibrations are measured with a transducer, preferably an accelerometer. Then, the signal is analogically integrated in real time, and the phase diagram is plotted. When the bearing is new, the first diagram (Fig. 9) corresponds to the healthy reference. Since we know that bearings have a nonlinear response, and that this response is the result of its stiffness dependency on frequency, we can monitor the phase diagram in order to "see" the instant when instabilities occur. In this way, if we permanently monitor the "shape" of the phase diagram, and we detect the appearance of instabilities, then we will be able to detect early faults. Fig.9 shows a phase diagram of a healthy bearing. In this figure, we can see four major loops, they correspond to the main frequencies, the unbalance load produces the external loop, and the other three are the mayor bearing frequencies. This diagram shows similar shapes at different time steps.

Fig. 10 shows the phase diagram of a damage bearing. Comparing both diagrams, it is clearly seen that bearing looses stability when there is a defect. This stability change can be detected with an appropriate electronic monitoring system.

3.5 Friction

Dry friction is an important source of mechanical damping in many physical systems. The viscous-like damping property suggest that many mechanical designs can be improved by configuring frictional interfaces in ways that allow normal forces to vary with displacement. The system is positively damped at all times and is clearly stable (Anderson & Ferri 1990) (Oden & Martins, 1985).

Distinctions between coefficients of static and kinetic friction have been mentioned in the friction literature for centuries. Euler developed a mechanical model to explain the origins of

frictional resistance. He arrived at the conclusion that friction during sliding motion should be smaller. The experiment proposed by Euler involved the sliding of a body down an inclined plane at slopes close to the critical slope at which sliding initiates. This, of course, would mean that, as soon as sliding initiates, a drop of friction force occurs, the difference between static and kinetic friction forces being responsible for the acceleration of the body down the inclined plane (stick-slip in sliding systems).

Phase Diagram, Experimental Data
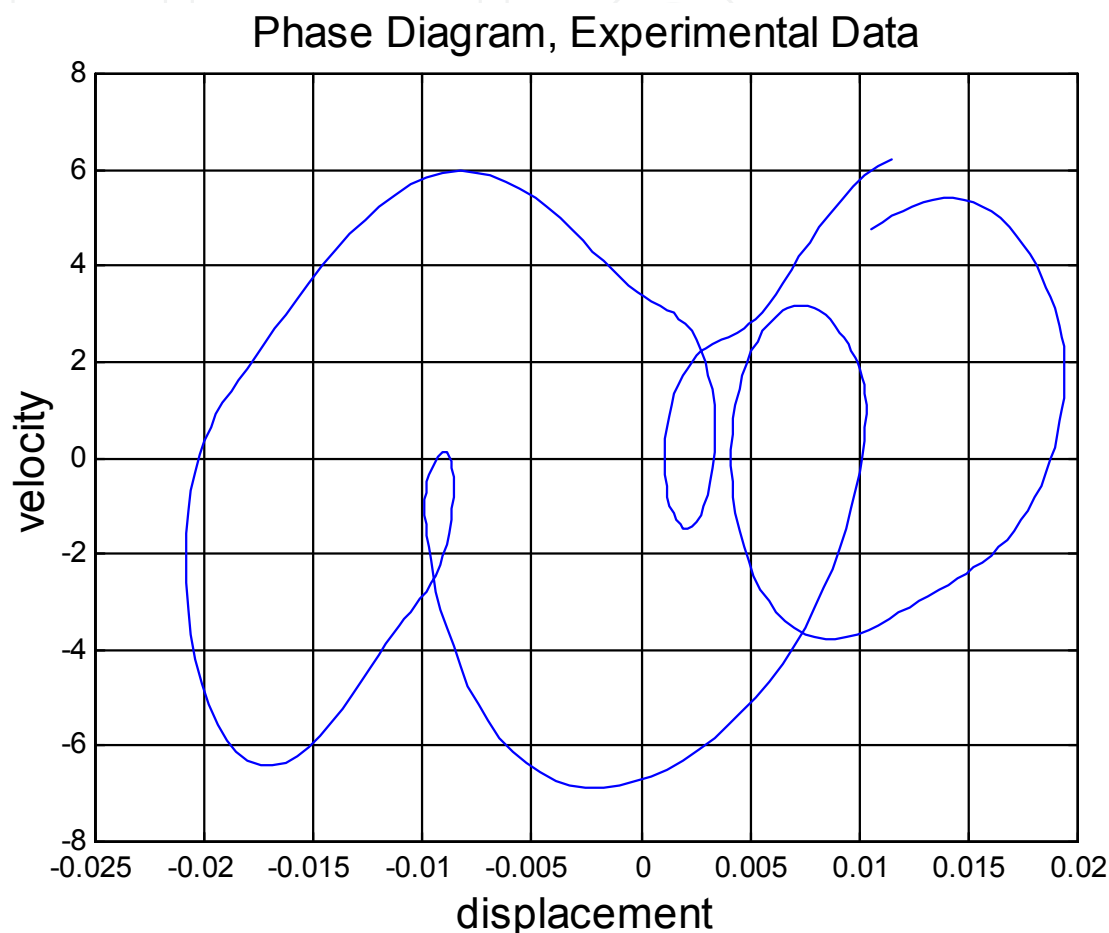
Fig. 9. Phase diagram of a healthy bearing

The distinction between static and kinetic friction was also a major topic of Coulomb's detailed experimental study. Coulomb's work is the first major reference dealing with the increase of the coefficient of static friction with increasing times of repose (stationary contact before the initiation of sliding). Coulomb observed a dependence of the kinetic friction on the sliding velocity and a dependence of the static friction on the time of repose. However, for dry metal-to-metal interfaces all those distinctions or variations were absent or negligible.

In general, the coefficient of kinetic friction would be small and increasing with sliding velocity at low velocities. Then, at some velocity, it would achieve a maximum value after which it would decrease with the increase of speed. The sliding process is not a continuous one; the motion proceeds by jerks. The metallic surfaces "stick" together until, as a result of the gradually increasing pull, there is a sudden break with a consequent very rapid "slip". The surfaces stick again and the process is repeated indefinitely. When the surfaces are of

the same metal, the behavior is somewhat different. Large fluctuations in the friction still occur but they are comparatively slow and very irregular. The average value of the frictional force is considerably higher than that found for dissimilar metals and a well-marked and characteristic track is formed during the sliding.
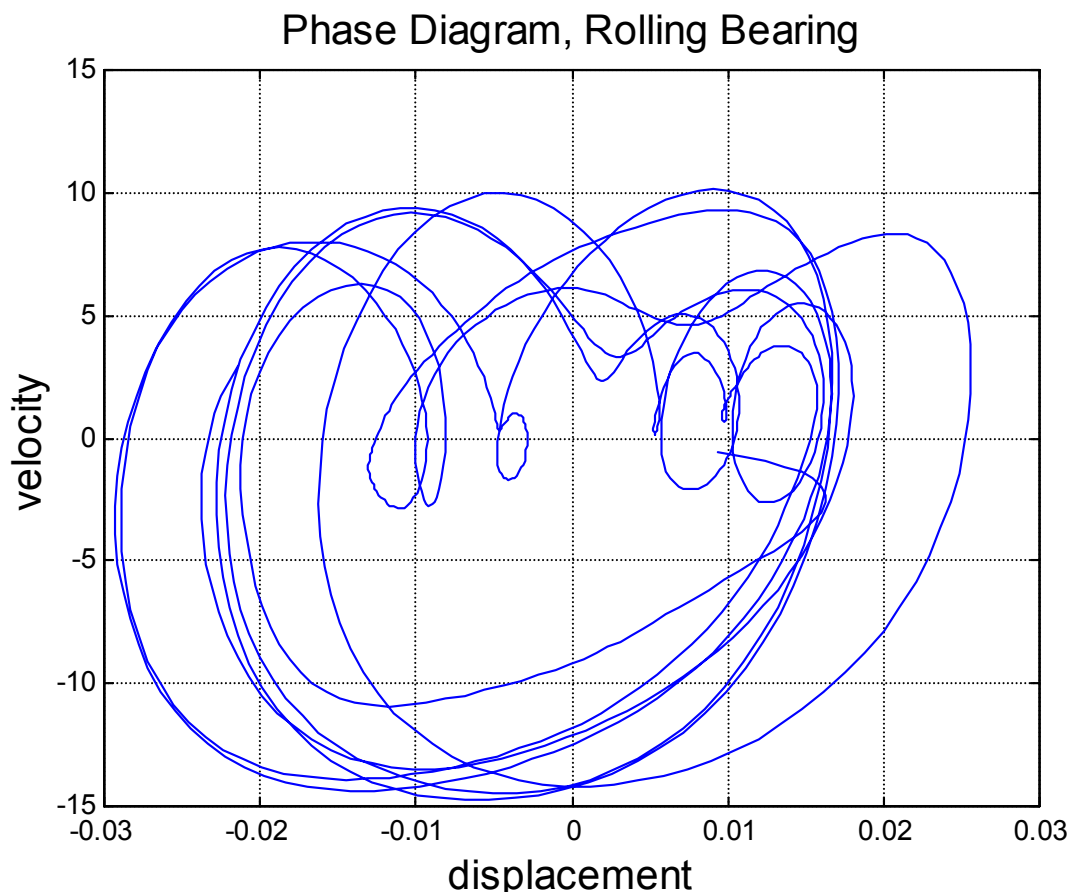

Fig. 10. Phase diagram of a damaged bearing.

It has also been observed that the frequency of the stick-slip motion increases with the increase of the driving velocity and that the maximum value of this frequency approaches the undamped natural frequency of the system, although in some cases the oscillation stops at a level well below that of the natural frequency.

The Martin model (Oden &Martins 1985) considers a two-degree-of-freedom system, where the normal force between the sliding block is its weight, and it is free to separate from the sliding surface upwards

$$F_\mu = \mu(y^2)sgn(\dot{x} - v) \,. \tag{29}$$

The dynamic behavior of a single-degree-of-freedom system with amplitude and rate dependant friction forces is presented. A system with amplitude-dependant friction is more likely to experience intermittent sticking. If the system sticks a significant amount of time, the energy dissipation capability may be degraded. Hence, special care is taken in this analysis to examine sticking conditions (in the case of gear teeth action sticky occurs only for very high contact stresses). In general sticking can occur only when the sliding velocity is zero.

The extended friction law is (Anderson &Ferri 1990):

$$F_\mu = \mu(C_0 + C_1|x| + C_2|\dot{x}|)sgn(\dot{x}) \qquad (30)$$

where x represents the sliding displacement, $\dot{x}$ represents the sliding velocity, C_0 is the normal force, C_1 is the friction interface amplitude, C_2 is the friction interface velocity and μ is the coefficient of friction (in general is the equivalent to the static coefficient of friction).
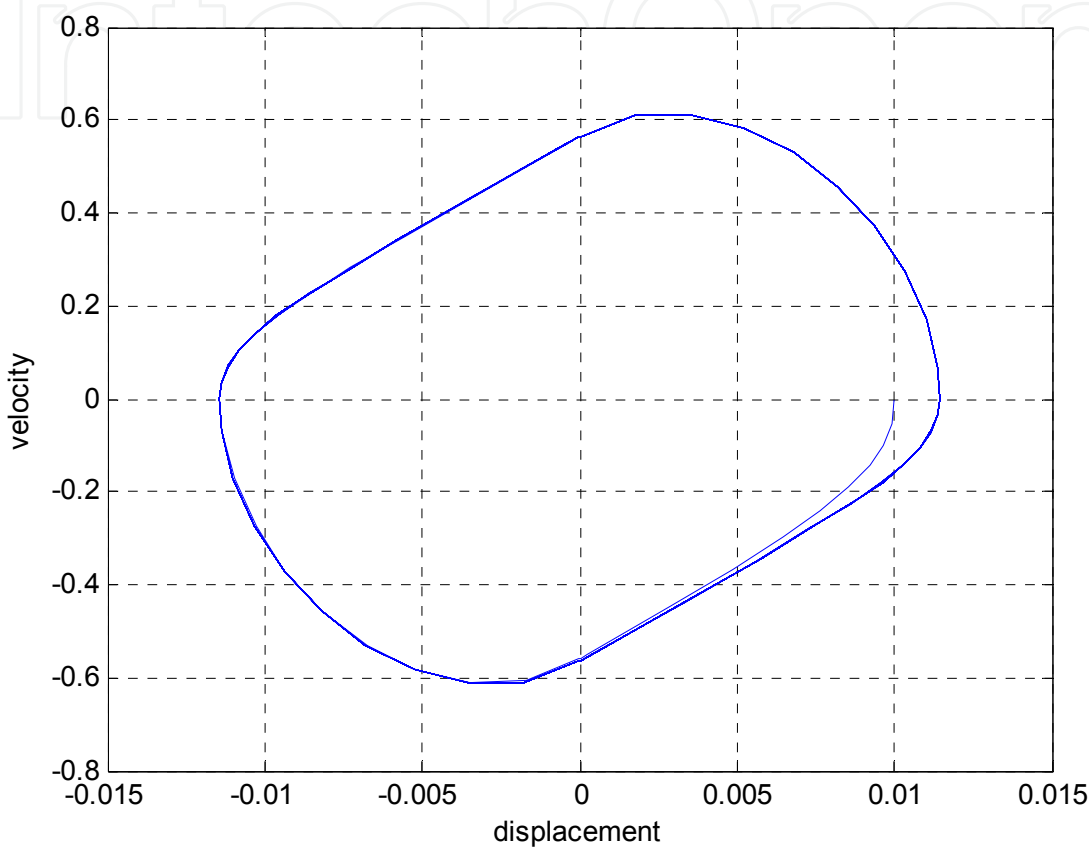

Fig. 11. Phase diagram for a single degree freedom model. Free vibration

The dynamic model for a single-degree-of-freedom system is represented as:

$$m\ddot{x} + c\dot{x} + kx + F_\mu = F_e\cos(\omega t). \qquad (31)$$

The system is positively damped at all times and it is clearly stable in the sense of Lyapunov. However the system is not asymptotically stable for $C_0 \neq 0$. This condition is identified from the phase diagram when $F_e = 0$ and the initial x=0.1.
The friction force has a particular behavior; it can be observed in Fig. 12.

3.6 Rubbing
One of the most interesting and practically important dynamic responses of rotor systems are caused by bearing clearances, which are mainly due to piecewise nature of stiffness characteristics. It is well known that dynamic interactions in such systems can lead to much more complex nonlinear behavior than in systems with smooth nonlinearities, including existence of grazing bifurcations and untypical routes to chaos such as blowout. In rotor
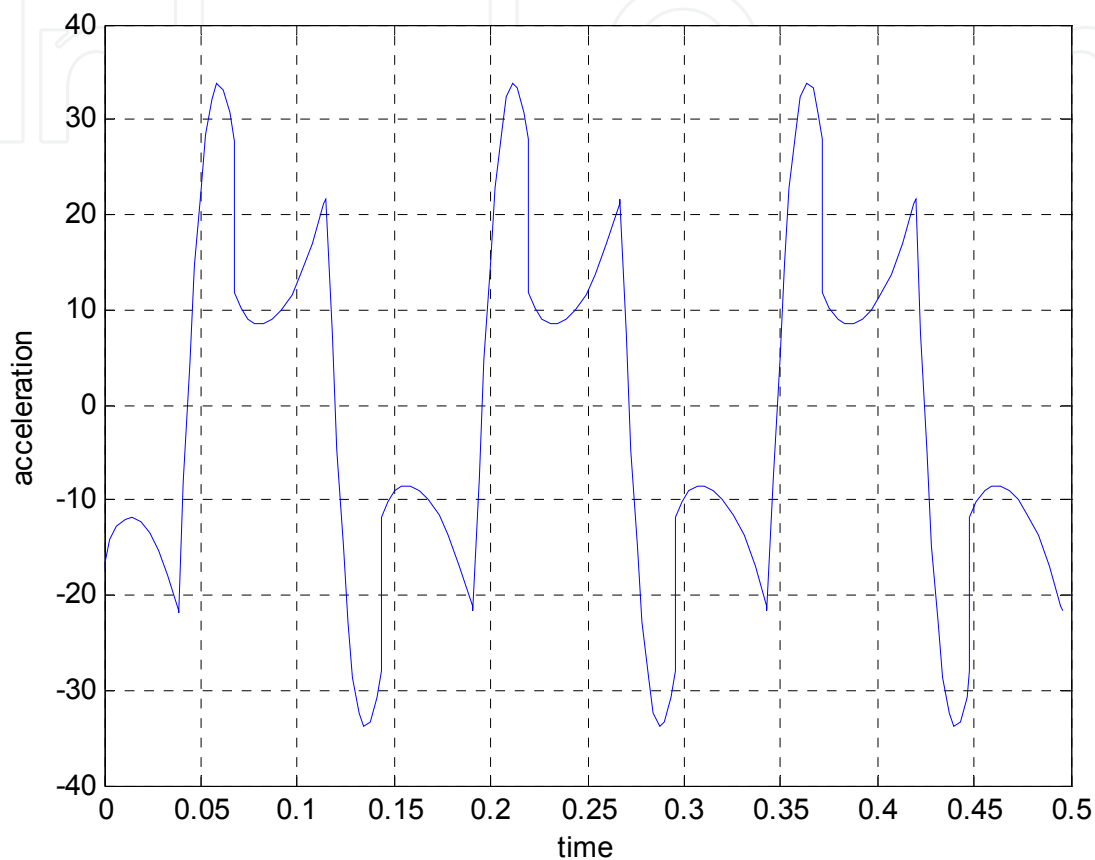
Fig. 12. Friction force produced by the general friction law

systems, such phenomena are caused by intermittent contacts between the components of the rotor system, which can lead to catastrophic failures. Therefore, it is vastly important to conduct experimental verifications in order establish credible mathematical models predicting complex dynamic responses of rotor systems.

There is a big difference between friction and rubbing. Whereas friction has a smooth phase diagram, rubbing develops a chaotic behavior. This chaotic behavior is associated with a sever stiffness discontinuity (Jauregui & Gonzalez 2009a; Rubio & Jauregui 2011). Pure friction acts as a damper and stabilizes the system, whereas, rubbing modifies the stiffness of the system. The stability pattern will depend on the hardness of the surface. If a rotor rubs a hard surface, the phase diagram will show a pattern similar to Fig. 13. If the rotor rubs a soft surface, the phase diagram will have a different pattern (Fig. 14).
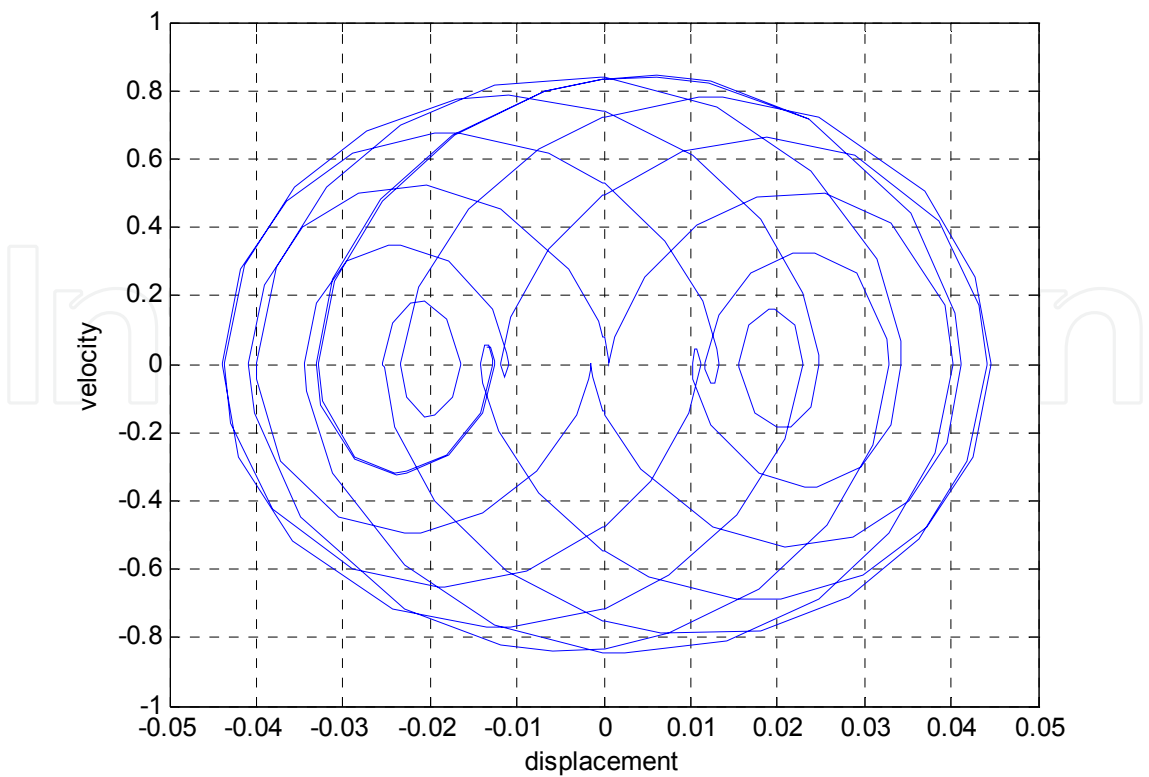
Fig. 13. Phase diagram for a rotor rubbing a hard surface
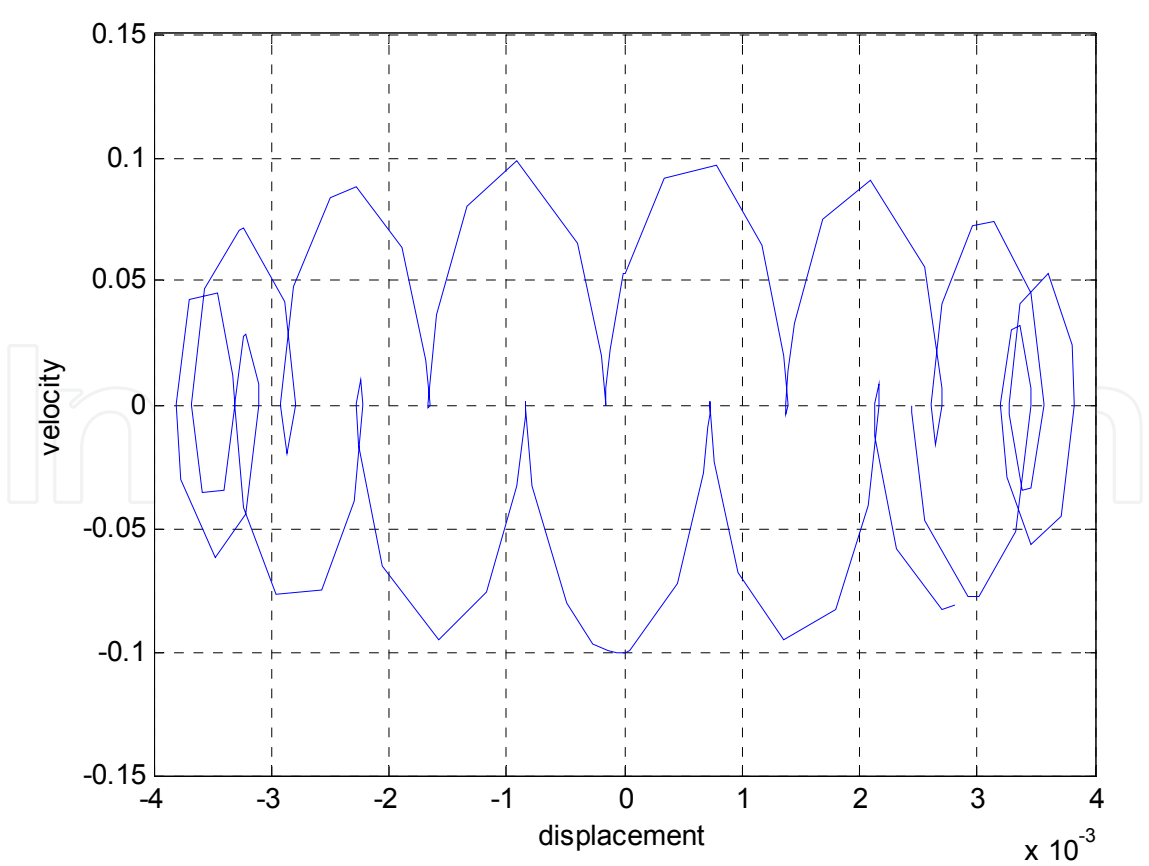

Fig. 14. Phase diagram for a rotor rubbing a soft surface

4. Conclusions

The phase diagram or phase space is a geometric representation of the Hamiltonian function of a dynamic system. It represents the relationship between the potential and kinetic energies at any time. Since the dynamic instability of a system will modify the trajectory of the phase space, the phase diagram will reflect any significant change in the Hamiltonian function. Thus, the phase diagram is a useful tool for predicting and monitoring nonlinear systems, and also it can identify transient responses. Linear systems have stable, well defined elliptical functions.

The phase diagram can be implemented into an electronic device, and it is possible to construct it in real time. The difficulty arises from its interpretation. Therefore, it is important to understand the phase diagrams of each system. It is known that there is no single model that can describe a nonlinear system. Some mechanical elements can be represented with certain models, but their dynamic response will depend not only on the model, but also in the system's sensibility to the nonlinear terms.

The phase diagram can be used to determine the system response and it can identify when a dynamic system becomes instable. For most nonlinear systems, the phase space changes from a smooth simple geometry, to a completely different pattern. Even more, under stable conditions, the phase space repeats its shape periodically, whereas under an unstable condition, the pattern changes as a function of time.

5. References

Kerschen, G., Worden, K., Vakakis, A. & Golinvala, J. (2006). Past, present and future of nonlinear system identification in structural dynamics, *Mechanical Systems and Signal Processing*, Vol. 20, pp 505–592

Masri, S., (1994). A hybrid parametric/nonparametric approach for the identification of nonlinear systems, *Probabilistic Engineering Mechanics,* Vol. 9, pp 47-57

Wiercigroch, M. & Pavlovskaia, E., (2008) Non-linear dynamics of engineering systems, *International Journal of Non-Linear Mechanics,* Vol. 43 pp 459 -461

Pai, F., (2007) Nonlinear vibration characterization by signal decomposition, *Journal of Sound and Vibration,* Vol. 307 pp 527–544

Yang, J., Zhang, Y. & Zhu, Y. (2007). Intelligent fault diagnosis of rolling element bearing based on SVMs and fractal dimension, *Mechanical Systems and Signal Processing* Vol. 21 pp 2012–2024

Li, C. & Qu, L. (2007) Applications of chaotic oscillator in machinery fault diagnosis, *Mechanical Systems and Signal Processing* Vol. 21 pp 257–269

Rüdinger, F. & Krenk, S., Non-parametric system identification from non-linear stochastic response, *Probabilistic Engineering Mechanics*, Vol. 16 pp 233-243

Schuëller, G. (1997) A State-of-the-Art Report on Computational Stochastic Mechanics, *Probabilistic Engineering Mechanics,* Vol. 12, No. 4, pp. 197-321

Vela, L., Jauregui, J., Rodriguez, E., & Alvarez, J. (2010) Using detrended fluctuation analysis to monitor chattering in cutter tool machines, *International Journal of Machine Tools & Manufacture* Vol. 50 pp 651–657

Modarres,Y., Chasparis,F., Triantafyllou, M., Tognarelli ,M. & Beynet, P. (2011) Chaotic response is a generic feature of vortex-induced vibrations of flexible risers, *Journal of Sound and Vibrations,* Article in press.

Liu, B., (2005) Selection of wavelet packet basis for rotating machinery fault diagnosis, *Journal of Sound and Vibration* Vol. 284 pp 567–582

Wang, G., Li, Y., & Luo, Z., (2009) Fault classification of rolling bearing based on reconstructed phase space and Gaussian mixture model, *Journal of Sound and Vibration* Vol.323 pp 1077–1089

Wang, Z., Akhtar, I., Borggaard, J., & Iliescu, T., (2011) Two-level discretizations of nonlinear closure models for proper orthogonal decomposition, *Journal of Computational Physics* Vol.230 pp 126–146

Ghafari, S., Abdel, E., Golnaraghi, F. & Ismail, F., (2010) Vibrations of balanced fault-free ball bearings, *Journal of Sound and Vibration* Vol. 329 pp 1332–1347

Karpenko, E., Wiercigroch, M., Pavlovskaia, E. & Neilson, R., (2006). Experimental verification of Jeffcott rotor model with preloaded snubber ring, *Journal of Sound and Vibration* Vol. 298 pp 907–917

Mevela,B. & Guyaderb, J. (2008) Experiments on routes to chaos in ball bearings, *Journal of Sound and Vibration* Vol. 318 pp 549–564

Nichols, J. (2003), Structural health monitoring of offshore structures using ambient excitation, *Applied Ocean Research* Vol. 25 pp 101–114

Jauregui, J. & Gonzalez, O., (2009a), *Mechanical Vibrations of Discontinuous Systems* (1st edition), Nova Science Publishers, ISBN: 978-1-60876-126-5, New York

Jauregui, J. & Gonzalez, O., (2009b),Non-linear vibrations of slender elements, In: *Mechanical Vibrations measurements, effects and control,* Sapri, R., pp 557-588, Nova Science Publishers, ISBN: 978-1-60692-036-7, New York

Chang, C., Strong nonlinearity analysis for gear-bearing system under nonlinear suspension -bifurcation and chaos, *Nonlinear Analysis: Real World Applications* Vol.11 pp 1760–1774

Andreaus, U. & Baragatti, P., (2011) Cracked beam identification by numerically analysing the nonlinear behaviour of the harmonically forced response, *Journal of Sound and Vibration* Vol. 330 pp 721–742

Machado, L., Lagoudas, D. & Savi, M., (2009) Lyapunov exponents estimation for hysteretic systems, *International Journal of Solids and Structures* Vol. 46 pp 1269–1286

Mazzillia, C., Sanches, C., Netoa, B., Wiercigrochb, M. & Keber, M., Non-linear modal analysis for beams subjected to axial loads: Analytical and finite-element solutions, *International Journal of Non-Linear Mechanics* Vol. 43 pp 551 – 561

Anderson, J., &. Ferri, A., (1990) Behavior of a single-degree-of-freedom-system with a generalized friction law, *Journal of Sound and Vibration* Vol. 140(2), pp 287-304

Oden, J., Martins, J., (1985) Models and computational methods for dynamic friction phenomena, *Computer methods in applied mechanics and engineering,* Vol. 52, pp 527-634

Rubio, E., Jauregui, J., (2011), Time-Frequency Analysis for Rotor-Rubbing Diagnosis, *Advances in Vibration Analysis Research*, Ebrahimi, F., ISBN 978-953-307-209-8 , InTech Publishers
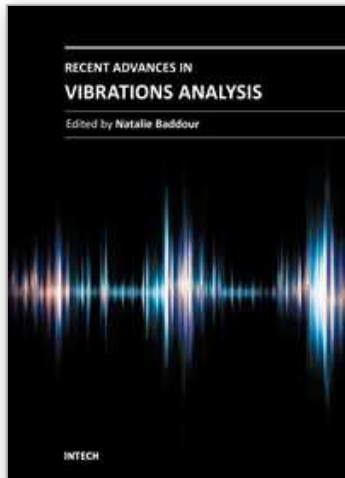
Recent Advances in Vibrations Analysis

Edited by Dr. Natalie Baddour

This book covers recent advances in modern vibrations analysis, from analytical methods to applications of vibrations analysis to condition monitoring. Covered topics include stochastic finite element approaches, wave theories for distributed parameter systems, second other shear deformation theory and applications of phase space to the identifications of nonlinearities and transients. Chapters on novel condition monitoring approaches for reducers, transformers and low earth orbit satellites are included. Additionally, the book includes chapters on modelling and analysis of various complex mechanical systems such as eccentric building systems and the structural modelling of large container ships.

How to reference

In order to correctly reference this scholarly work, feel free to copy and paste the following:

Juan Carlos Jáuregui (2011). Phase Diagram Analysis for Predicting Nonlinearities and Transient Responses, Recent Advances in Vibrations Analysis, Dr. Natalie Baddour (Ed.), ISBN: 978-953-307-696-6, InTech, Available from: http://www.intechopen.com/books/recent-advances-in-vibrations-analysis/phase-diagram-analysis-for-predicting-nonlinearities-and-transient-responses

INTECH
open science | open minds